Atmospheric
Chemistry
and Physics

Supplement of

A self-consistent, multivariate method for the determination of gas-phase rate coefficients, applied to reactions of atmospheric VOCs and the hydroxyl radical

Jacob T. Shaw et al.

Correspondence to: Jacqui F. Hamilton (jacqui.hamilton@york.ac.uk)

Supplementary Information

On the establishment of laminar flow

The Reynold's number for the reactor was calculated using Eq. S1. This was done for the two different flows through the reactor; the first, initial flow of 2000 sccm of humidified N_2 and the second, total flow of 3000 sccm humidified N_2 and

5   VOC mixture.

$$Re = \frac{\rho u D_h}{\mu} = \frac{u D_h}{\nu} = \frac{Q D_h}{\nu A} \qquad\qquad \text{Eq. S1}$$

The initial flow of humidified N_2 has Re = 88, with an entrance length of 0.1 m. The flow after the injection of the

10   VOC mixture has Re = 132 and an entrance length of 0.2 m. The low values of Re suggest that laminar flow is established within the reactor, both initially and after injection of the VOCs. However, these calculations do not take into account that the VOC mixture is injected perpendicular to the main flow, which is likely to cause considerable turbulence.

Kinetic simulations of poor mixing resulting in non-linearity

Simple kinetic simulations were conducted using Kintecus (Ianni, J. C., 2017) and incorporated the OH + VOC

15   reaction for each VOC in Mixture 1 and simple HO_x chemistry (OH + OH, OH + HO_2, HO_2 + HO_2). The initial [HO_2] was set to be equivalent to the initial [OH] for each simulation. This is likely to hold roughly true in the experiment, as photolysis of H_2O produces both OH and H radicals. The H radicals are expected to quickly react with residual O_2 to rapidly form HO_2.

To simulate incomplete mixing of OH, the reactor was divided into three distinct theoretical air parcels; one where 1/3 of the [VOC] is exposed to a low [OH], one where 1/3 [VOC] is subjected to a high [OH] and one where 1/3 [VOC] is

20   exposed to a level of [OH] between the these two high and low values. The depletion factors calculated from the VOC concentrations in each of these air parcels can be plotted separately, or the concentrations summed together to yield a depletion factor for the final concentration. The average depletion factor is more representative of what is actually measured by the GC-MS, assuming that thorough mixing of all air parcels takes places after the reactions with OH have occurred.

Figure S1 shows that in each of these air parcels, the VOCs are depleted relative to their rate coefficients. The adjusted

25   R^2 values for each of the three linear regressions is 1.0.

However, if the VOC concentrations in each section of the reactor are summed before the depletion factor is calculated, as happens prior to sampling, the resulting plot against rate coefficient is curved, as shown in Fig. S2. This curvature still occurs at higher [VOC] but is much less pronounced, to the extent that the relationship can be assumed to be linear. Figure S3 shows the same simulation but for a [VOC] of 10 ppb, or OH reactivity of 290 s^{-1}. Note that the model reproduces the

discrepancy in depletion factor observed experimentally and that the curvature is only noticeable in cases where the depletion factor is greater than 0.4

Whilst this artefact of the experiment does represent a limit, at least in terms of sensitivity towards measuring rate coefficients towards the faster end of the reactivity spectrum, it does affect measurements made for VOCs with a depletion factor less than 0.4. As mentioned before, if a consistent function can be plotted through the data and an unknown is interpolated using that function, relative rate conditions should still apply.

Ianni, J. C.: Kintecus, Windows Version 6.01, 2017, www.kinetcus.com

Table S1 Estimated range in total VOC concentration and total OH reactivity of each mixture injected into the reactor.

Mixture no.	total [VOC] / ppb	total OH reactivity / s^{-1}
1	22-110	50-250
2	22-110	20-100
3	25-100	30-130

Table S2 O$_3$ + VOC literature data for compounds in the ambient air analysis.

compound	literature[a] k_{O3} / 10^{-17} cm^3 molecule^{-1} s^{-1} 298 K
tridecane	$< 1 \times 10^{-6}$
isoprene	1.27
styrene	1.70
3-ethyltoluene	$< 1 \times 10^{-3}$
dodecane	$< 1 \times 10^{-6}$
1,2,3-trimethylbenzene	$< 1 \times 10^{-3}$
1,2,4-trimethylbenzene	$< 1 \times 10^{-3}$
naphthalene	0.02
2-ethyltoluene	$< 1 \times 10^{-3}$
n-decane	$< 1 \times 10^{-6}$
ethylbenzene	$< 1 \times 10^{-3}$
n-heptane	$< 1 \times 10^{-6}$
n-propylbenzene	$< 1 \times 10^{-3}$
toluene	$< 1 \times 10^{-3}$
benzene	$< 1 \times 10^{-3}$
isopropylbenzene	$< 1 \times 10^{-3}$
n-hexane	$< 1 \times 10^{-6}$
ethyl acetate	
dichloromethane	

[a] Atkinson and Arey, 2003
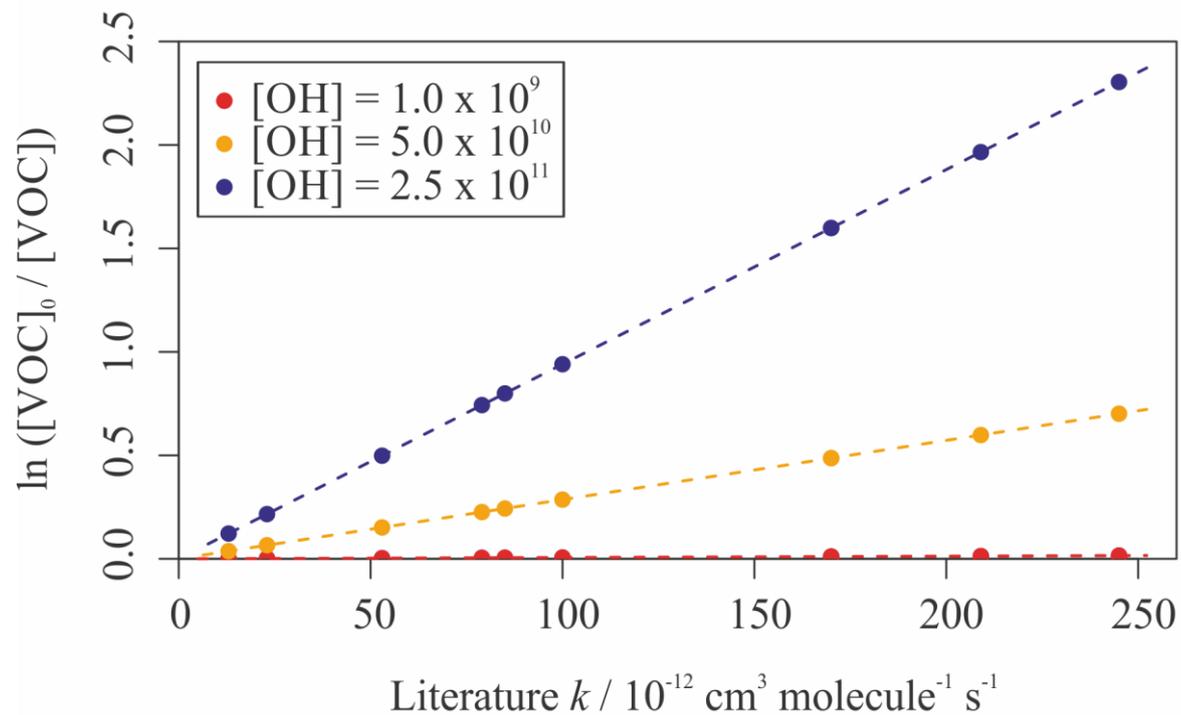
Figure S1 Simulated depletion factors for Mixture 1 (OH reactivity = 50 s^{-1}) plotted against literature rate coefficients. Here, three air parcels are simulated separately, with each air parcel containing 1/3 [VOC] and exposed to different [OH].
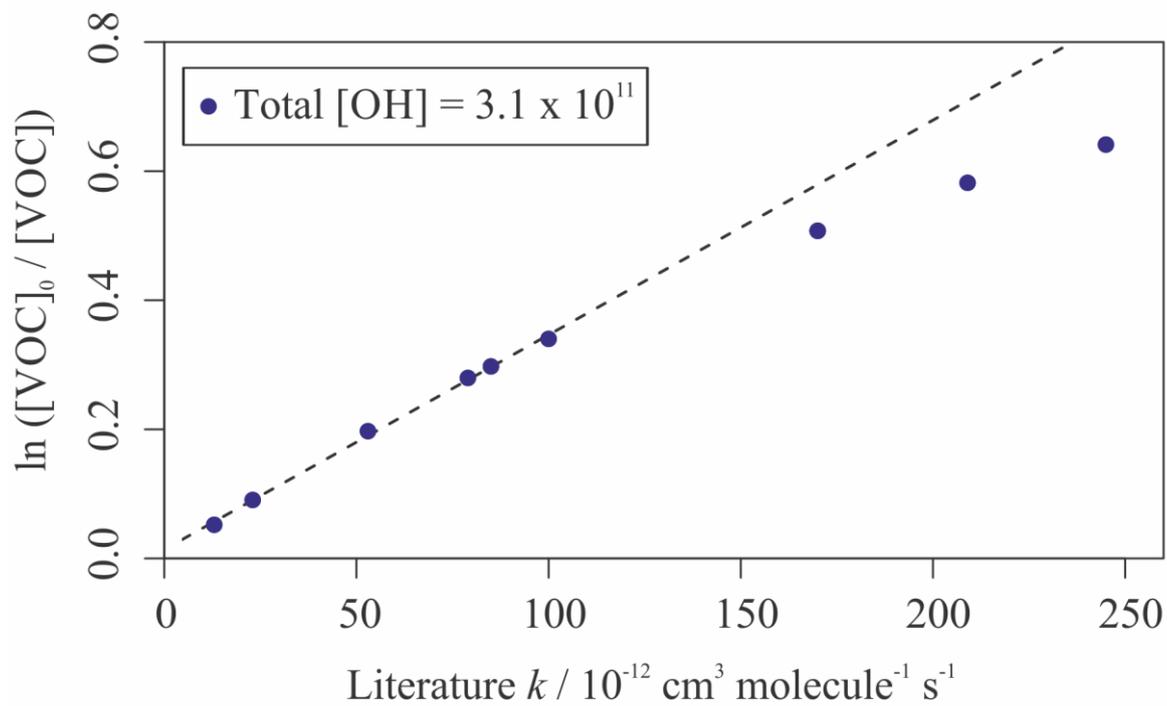
Figure S2 Simulated depletion factors for Mixture 1 (OH reactivity = 50 s⁻¹) plotted against literature rate coefficients. Here, the concentrations of the VOCs in each of the three simulated air parcels (see Fig. S1) are summed and the depletion factor for the final concentration is plotted against literature rate coefficient. Note that the relationship between depletion factor and k is no longer linear, although a straight line can be plotted through the data with a depletion factor of less than 0.4
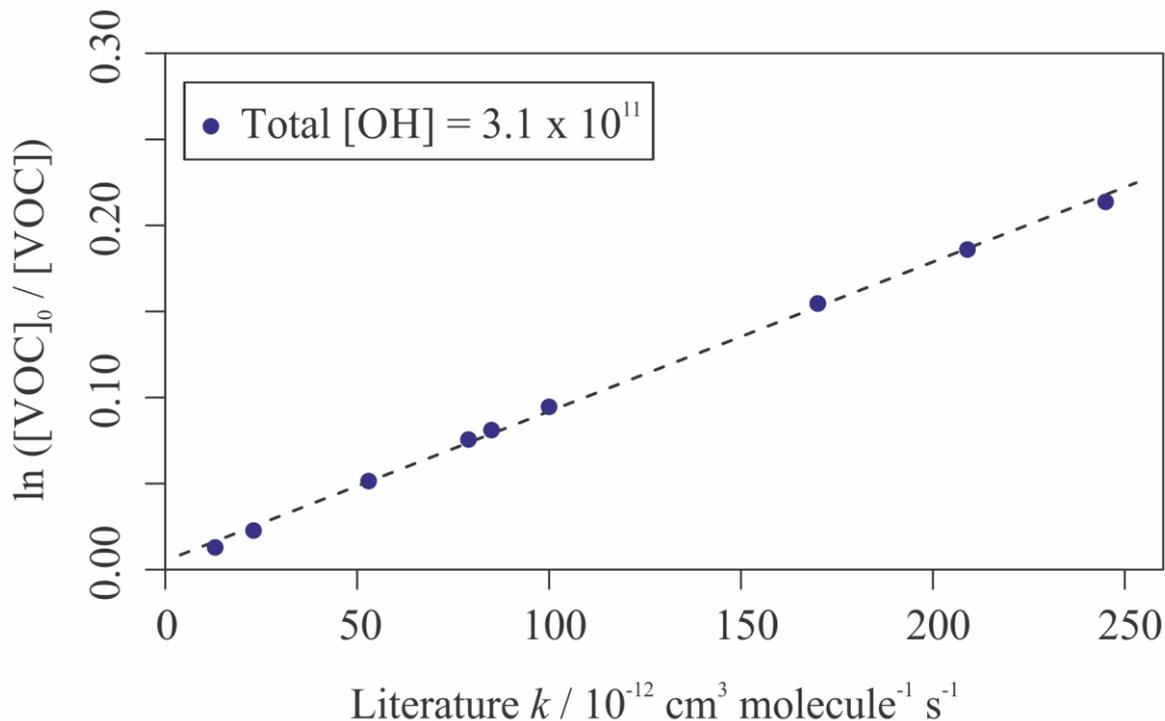
5

Figure S3 Simulated depletion factors for Mixture 1 (OH reactivity = 290 s⁻¹) plotted against literature rate coefficients. Here, the concentrations of the VOCs in each of the three simulated air parcels (see Fig. S1) are summed and the depletion factor for the final concentration is plotted against literature rate coefficient. Note that the relationship between depletion factor and k is no longer linear.
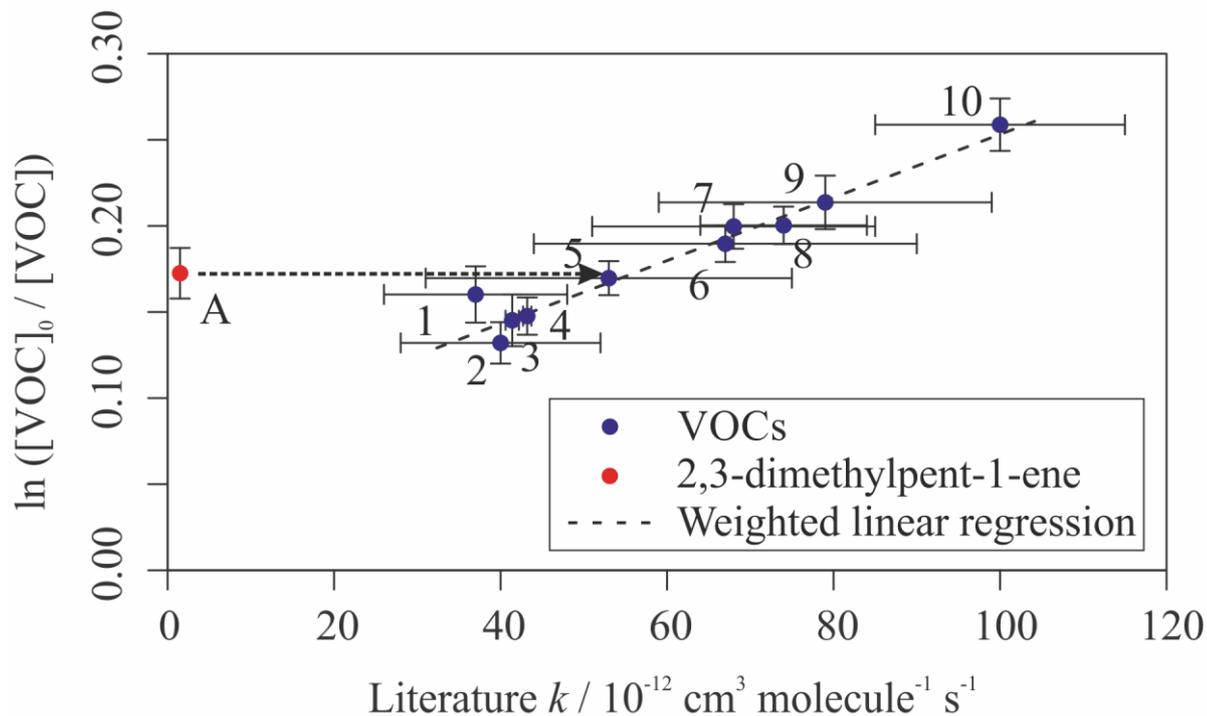
5

Figure S4 Relative rate plot for Mixture 2 (OH reactivity = 30 s^{-1}) at 295 K. Compounds with a known rate coefficient are plotted using literature values. Error bars on the y-axis, equal to one standard error, are calculated by combining the standard error in peak areas for 6 lamp off samples and 6 lamp on samples. Error bars on the x-axis are approximately ± 20-30% and account for deviations from the line. A weighted linear fit was used to generate the slope with a value of OH_{exp} = 1.8 (± 0.14) × 10^9 molecules cm^{-3} s and R^2 of 0.95. Data for 2,3-dimethylpent-1-ene, which has no literature k value, was not used in the calculation of the fit. Identity of VOCs: 1, 1-hexene; 2, 1-heptene; 3, 1-octene; 4, 1-nonene; 5, α-pinene; 6, cyclopentene; 7, cyclohexene; 8, cycloheptene; 9, β-pinene; 10, isoprene.
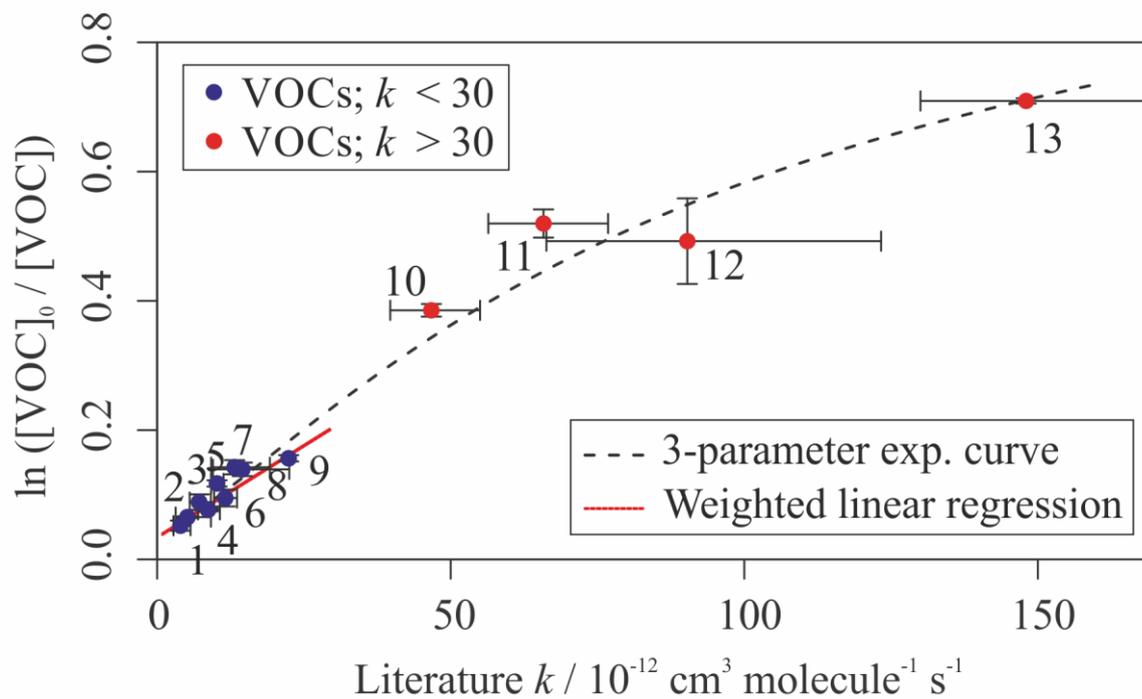
Figure S5 Relative rate plot for Mixture 3 (OH reactivity = 60 s-1) at 323 K. Compounds with a known rate coefficient are plotted using literature k (323 K) values. Error bars on the y-axis, equal to one standard errors, are calculated by combining the standard error in peak areas for 5 lamp off samples and 5 lamp on samples. The black dashed line shows the relationship observed when VOC concentrations are low, modelled by an exponential cumulative distribution. A weighted linear fit was used to generate the red slope (R2 of 0.976) for VOC with k (323 K) less than 30 × 10-12 cm3 molecule-1 s-1. Identify of VOCs: 1, 2,2,3-trimethylbutane; 2, toluene; 3, n-heptane; 4, n-octane; 5, n-nonane; 6, n-decane; 7, cycloheptane; 8, cyclooctane; 9, naphthalene; 10, α-pinene; 11, β-pinene; 12, isoprene; 13, limonene.
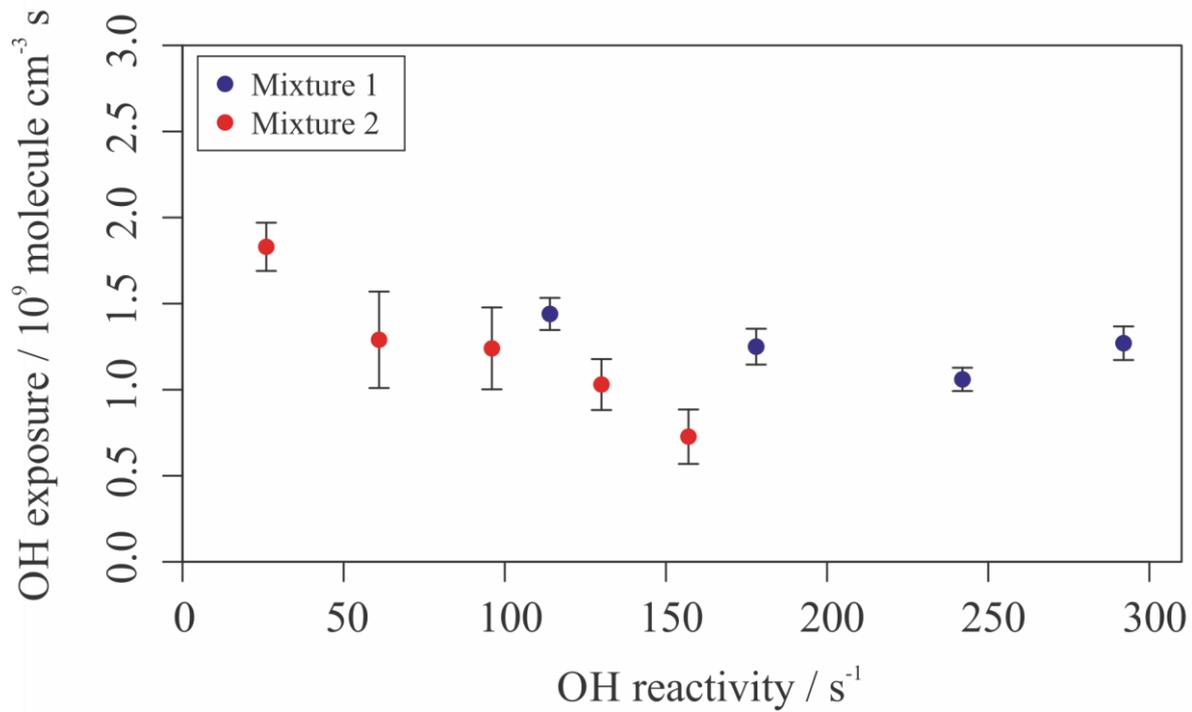
Figure S6 Plot of OH exposure against estimated OH reactivity for the synthetic gas mixtures 1 and 2 showing the trend in OH exposure with increasing OH reactivity.